

Effects of intake air conditions and micro-pilot (MP) injection timing on micro-pilot dual fuel (MPDF) combustion characteristics in a single cylinder optical engine

Minhoo Choi, Sungwook Park*

School of Mechanical Engineering, Hanyang University, 222 Wangsimni-ro, Seongdong-gu, Seoul 04763, Republic of Korea

ARTICLE INFO

Keywords:

Micro-pilot dual fuel
Misfiring
Knocking combustion
Combustion variation
Operating parameters

ABSTRACT

The effects of intake air conditions and micro-pilot injection timing on the characteristics of micro-pilot dual fuel combustion were examined to enhance the combustion stability in marine engines. A minimum amount of diesel fuel was injected as the ignition source, and most of the fuel energy was obtained from methane gas. First, the intake air flow rate was varied. In addition, the methane gas flow rate and micro-pilot injection timing were changed depending on the intake air flow rate. Second, the micro-pilot injection timing was varied under intake air temperatures of 35 °C and 55 °C. The intake air and methane gas flow rates were maintained. Results indicated that increasing the intake air and methane gas flow rates promoted autoignition in the end-gas region. Nevertheless, the standard deviation of the peak cylinder pressure was within 3.1 bar. Under the intake air temperature of 35 °C, advancing and retarding the micro-pilot injection led to misfiring, which increased the standard deviation of the peak cylinder pressure to 10.2 bar and 9.6 bar, respectively. Knocking combustion was occurred when the micro-pilot injection was retarded under the intake air temperature of 55 °C. This phenomenon increased the standard deviation of the peak cylinder pressure to 6.9 bar. Premixed ignition in the end-gas region combustion corresponded to the optimal engine operating conditions for marine engines because of the low combustion variation even under high cylinder pressures of approximately 170 bar to 220 bar. However, high NO_x emissions occurred under these conditions.

1. Introduction

Compression ignition (CI) engines based on diesel fuel generate considerable power and exhibit a high efficiency owing to the application of a high compression ratio and turbocharger [1–3]. Therefore, CI engines have been widely applied in various industrial fields. CI engines are essential for the propulsion of large vessels that require the generation of stable and high engine power. However, the harmful materials generated by CI engines have emerged as global issues in recent decades. In particular, owing to the use of low-quality fuels such as heavy fuel oil (HFO) and marine diesel oil (MDO) in marine engines, a large amount of nitrogen oxides (NO_x), sulfur oxides (SO_x), and particulate matter (PM) is produced [4–6]. To alleviate the problems caused by such emissions, the International Maritime Organization (IMO) has established emissions regulations for vessels, which mainly restrict the NO_x emissions and sulfur concentration in fuels [6,7]. Moreover, the emission control area (ECA) is being planned to be expanded to the Mediterranean,

Australia, and east Asia [7]. Many studies have been performed to address the strengthened regulations. An effective solution is the use of natural gas for marine engines. Natural gas mostly consists of methane (CH₄) gas [8]. CH₄ gas, which has the lowest carbon number among the hydrocarbon fuels and a simpler molecular structure, corresponds to a smaller amount of SO_x and PM emissions. Furthermore, CH₄ gas and air form a homogeneous mixture, which leads to low-temperature combustion [9]. Consequently, the amount of NO_x emissions, mainly generated by diffusion combustion, is dramatically decreased [10]. To effectively use CH₄ gas in marine engines, various dual fuel combustion technologies have been researched. Among these technologies, the focus of this study is micro-pilot dual fuel (MPDF) combustion. In dual fuel combustion, the characteristics of fuels determine the fuel supply method and purpose [11]. An extremely small amount of highly reactive fuel (diesel fuel) is directly injected into the combustion chamber during the compression stroke and used as an ignition source. Moreover, a large amount of gaseous fuel, which has low reactivity, is supplied to the engine through the intake port as a primary energy source. In MPDF

* Corresponding author.

E-mail address: parks@hanyang.ac.kr (S. Park).

<https://doi.org/10.1016/j.enconman.2022.115281>

Received 16 November 2021; Received in revised form 31 December 2021; Accepted 21 January 2022

Available online 2 February 2022

0196-8904/© 2022 The Author(s).

Published by Elsevier Ltd.

This is an open access article under the CC BY-NC-ND license

(<http://creativecommons.org/licenses/by-nc-nd/4.0/>).

Nomenclature*Abbreviations*

aSOE	After start of energization
aTDC	After top dead center
bTDC	Before top dead center
CA	Crank angle
CH ₄	Methane
C ₂ H ₆	Ethane
C ₃ H ₈	Propane
C ₄ H ₁₀	Butane
CI	Compression ignition
CO ₂	Carbon dioxide
ECA	Emission control area
EGR	Exhaust gas recirculation
H ₂	Hydrogen

HFO	Heavy fuel oil
IMO	International Maritime Organization
IMEP	Indicated mean effective pressure
LHV	Lower heating value
MDO	Marine diesel oil
MFB	Mass fraction burned
MP	Micro-pilot
MPDF	Micro-pilot dual fuel
NOx	Nitrogen oxides
PM	Particulate matter
PREMIER	Premixed mixture ignition in the end-gas region
RPM	Rotate per minute
SI	Spark ignition
SOx	Sulfur oxides
TDC	Top dead center
THC	Total hydrocarbon

Table 1
Specifications of engine and fuels [26].

Item	Description	
Engine type	Compressed ignition	
Compression ratio	17.0	
Bore (mm)	107	
Stroke (mm)	126	
Connecting rod (mm)	200	
Displacement volume (L)	1.1	
Number of injector nozzle holes	7	
Nozzle hole diameter (mm)	0.174	
Autoignition point of fuels (°C)	210 (Diesel)	358 (CH ₄)
LHV of fuels (MJ/kg)	45.4 (Diesel)	55.6 (CH ₄)

combustion, the fuel energy is mainly extracted from the gaseous fuel, and thus, this combustion method can effectively satisfy the emissions regulations.

Nevertheless, MPDF combustion involves high cycle-to-cycle variation compared with conventional CI engines that mainly use diesel fuel. This high cycle-to-cycle variation can be attributed to two factors. First, the presence of turbulent flow increases the combustion variation in MPDF combustion. Because an extremely small amount of diesel fuel is used in MPDF combustion, premixed combustion occurs in a dominant manner. As in the case of spark ignition (SI) engines, the turbulent flow randomly affects the flame propagation speed, leading to high cycle-to-cycle variation [12]. Choi et al. [13] investigated the effects of turbulent flow on dual fuel combustion variation under different fuel mixture ratios. The authors noted that as the gaseous fuel mixture ratio increases, the diffusion combustion transforms to premixed combustion, and the turbulent flow significantly increases the combustion variation under premixed combustion compared to that under diffuse combustion. Duraisamy et al. [14] performed engine experiments by considering different methanol and diesel mixture ratios for various engine operating loads. The authors reported that the cycle-to-cycle variation is proportional to the methanol mixture ratio at all engine operating loads.

Second, the combustion variation can be changed depending on the MPDF combustion forms. Among them, misfiring and knocking combustion leads to high combustion variation [15,16]. According to Lee et al. [17], the lack of an ignition source leads to misfiring, which deteriorates the combustion stability and thermal efficiency. Azimov et al. [18] defined the phenomenon of autoignition in the end-gas region under MPDF combustion as premixed ignition in the end-gas region (PREMIER) combustion. The authors reported that autoignition does not occur in the end-gas region under a low engine operating load. As the engine operating load increases, PREMIER combustion occurs, followed

by knocking combustion. Kawahara et al. [19] performed optical engine experiments to verify the differences between PREMIER and knocking combustion. The authors observed that knocking combustion can be attributed to the unpredictable autoignition in the combustion chamber. Furthermore, it is reported that while the PREMIER combustion maintains the low combustion variation, the knocking combustion leads to high combustion variation.

MPDF combustion characteristics are primarily affected by the engine operating parameters. Many researchers have performed various parametric studies. Poonia et al. [20] highlighted that increasing the intake air temperature promotes the MPDF combustion, resulting in decreased combustion duration. Meng et al. [21] changed the intake air pressure while kept the same fuel injection timing and dual fuel injection quantity. According to their research, increasing intake air pressure apparently advances the combustion phase, improving or deteriorating thermal efficiency depending on the dual fuel mixture ratio. Several researchers examined the effects of MP injection on the combustion characteristics [22–24]. It was reported that the MPDF combustion form depends on the MP injection timing, and knocking combustion occurs in cases involving advancing MP injection timing. Shim et al. [25] indicated that a lean equivalence ratio and high exhaust gas recirculation (EGR) ratio cause misfiring, leading to combustion instability and production of incomplete combustion materials. Conversely, Zheng et al. [8] reported that the peak cylinder pressure and exhaust gas temperature are proportional to the equivalence ratio.

In addition to engine operating parameters, the composition of gaseous fuel affects the MPDF combustion characteristic. The octane number represents the anti-knocking property of fuels. CH₄ gas exhibits a high anti-knocking capability owing to a high octane number. In contrast, the use of ethane (C₂H₆), propane (C₃H₈), and butane (C₄H₁₀) gases, which have low octane numbers, leads to knocking combustion [26]. Although CH₄ gas accounts for the largest proportion of natural gas, the inhomogeneity of natural gas may lead to variations in the octane number, causing knocking combustion to occur even under the same engine operating conditions. Therefore, hydrogen (H₂) gas, which has a higher anti-knocking property than CH₄ gas, has been introduced to dual fuel combustion engines to prevent the occurrence of knocking combustion [26,27]. In the combustion chamber, carbon dioxide (CO₂) gas dramatically decreases the combustion temperature owing to its large heat capacity. Therefore, CO₂ gas effectively prevents knocking combustion by reducing combustion temperature but excessive concentration of CO₂ gas lead to misfiring [25].

The abovementioned studies highlight the importance of preventing misfiring and knocking combustion for reducing combustion variation. Although the effects of various parameters on MPDF combustion characteristics have been extensively analyzed, only a few researchers have

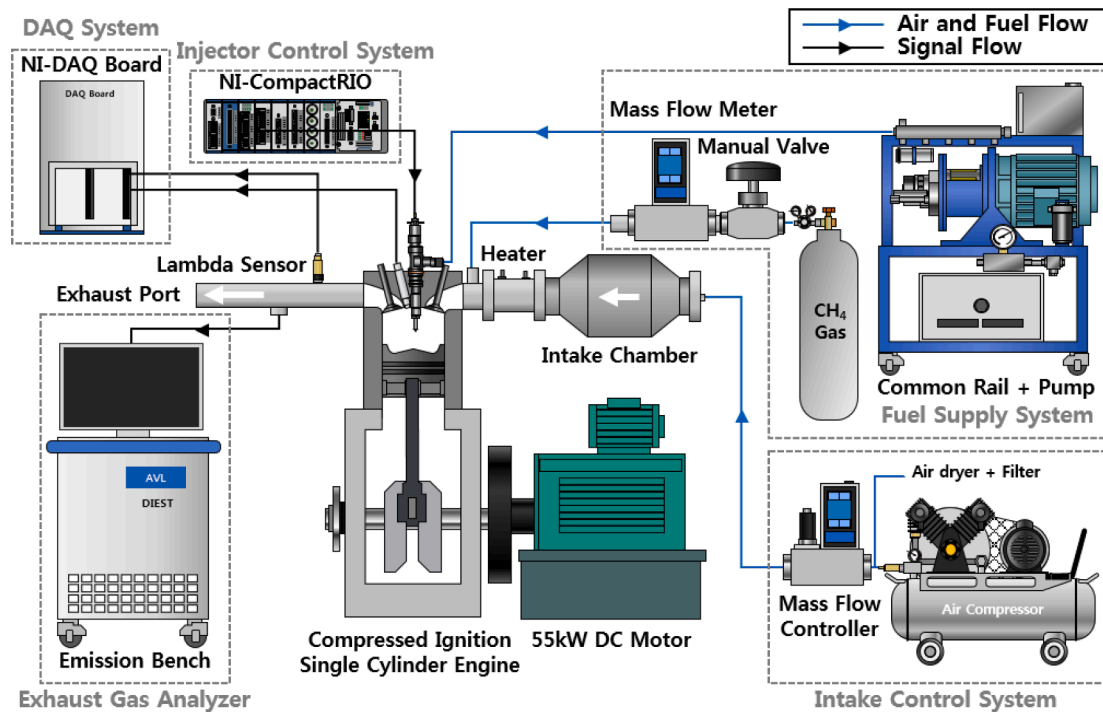


Fig. 1. Schematic of metal engine.

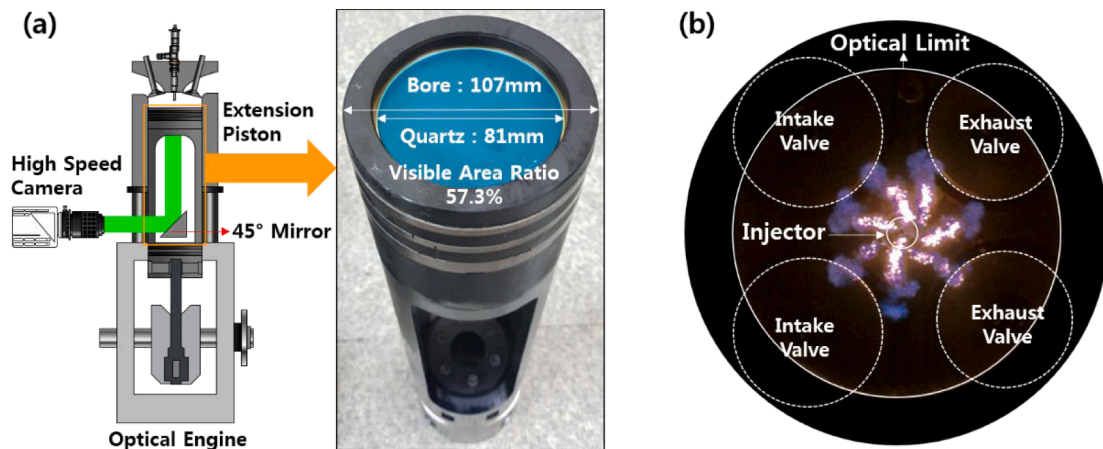


Fig. 2. (a) Schematic of optical engine and (b) bottom view of combustion.

comprehensively focused on the effects of engine operating parameters on MPDF combustion characteristics for preventing high combustion variation. In addition, the quantitative analysis of MPDF combustion is limited, which renders it challenging to distinguish the MPDF combustion forms. Considering these aspects, this study was aimed at analyzing the effects of intake air conditions, specifically, the intake air flow rate and temperature, and MP injection timing, on the characteristics of MPDF combustion. Moreover, the optimal engine operating conditions to reduce the combustion variation were derived.

2. Experimental method

2.1. Experimental setup

The specifications of engine and fuels are listed in Table 1 [26]. In practice, it is almost impossible to perform experiments on marine engines. Therefore, in this study, experiments were performed on the largest possible engine among onshore engines. Although the volumetric

size of the engine used in this study was smaller than that of marine engines, it was considered that the effects of engine operating parameters on the MPDF combustion characteristics could be analyzed. In particular, a compressed ignition single cylinder engine with a combustion chamber volume of 1.1 L and compression ratio of 17.0 was used. Because the single cylinder engine had only one cylinder, the errors caused by interference between cylinders and variations in intake flow could be eliminated. Fig. 1 shows a schematic of the metal engine. The experimental apparatus consisted of several systems. A 55 kW DC motor was used to operate the single cylinder engine at a constant speed. In addition, various systems were introduced to enable stable engine operation and data acquisition during the engine experiment. The intake control system was composed of an air compressor, a mass flow controller, an air dryer, an intake chamber and a heater. This system supplied a constant amount of dry air to the engine. The intake chamber was installed to minimize the fluctuation caused by the opening and closing of the intake valve, and a heater maintained the intake air temperature during the engine experiment. The fuels used in this study

Table 2
Combustion image acquisition conditions.

Item	Description
Lens diameter (mm)	105
Image acquisition speed (frame/s)	5,400
Camera resolution (height × width)	832 × 800
Exposure time (μs)	140
Pixel per length (pixel/mm)	7.32

Table 3
Reference experimental conditions.

Item	Description
Engine speed (RPM)	900
MP injection pressure (bar)	500
MP injection duration (ms)	0.3
LHV of MP (J/cycle)	45.8
Lambda (1/equivalence Ratio)	2.0
Intake air temperature (°C)	35
Coolant temperature (°C)	80
Oil temperature (°C)	80

Table 4
Experimental conditions for intake air flow rate.

Item	Description						
Engine type	Metal engine						
Intake air flow rate (L/min)	500	550	600	650	700	750	800
CH ₄ gas flow rate (L/min)	26.3	28.9	31.5	34.1	36.8	39.4	42.0
MP injection timing (CA, bTDC)	11	13	15	18	21	24	27

Table 5
Experimental conditions for MP injection timing.

Item	Description		
Engine type	Metal Engine	Optical Engine	Metal Engine
Intake air flow rate (L/min)	800	500	800
CH ₄ gas flow rate (L/min)	42.0	26.3	42.0
Intake air temperature (°C)	35	35	55
MP injection timing (CA, bTDC)	36, 33, 30, 27, 24, 21, 18	17, 14, 11, 8, 5	30, 27, 24

were diesel and CH₄ gas, and different types of supply equipment were used considering the fuel characteristics. The flow rate of CH₄ gas was controlled using a mass flow meter and manual valve to prevent unpredictable and/or excessive CH₄ gas supply. CH₄ gas was supplied to the engine through a flexible pipe connected to the intake port. A common rail and fuel pump supplied the diesel fuel to the injector at a constant pressure. The diesel fuel was injected to the combustion chamber through the center mounted injector. The NI-CompactRIO system equipped with the power train module controlled the diesel fuel injection timing and quantity. The exhaust gas analyzer measured the NO_x level and total hydrocarbon content (THC) during the engine experiment. The measured experimental data, which contained the combustion chamber pressure, lambda value, and intake flow rate and temperature were saved through the NI-DAQ Board. To address experimental variations, 100 cycles of experimental data were acquired and averaged. Optical devices were installed on the single cylinder engine to obtain combustion images to facilitate the experimental analysis. Fig. 2 (a) shows a schematic of the optical engine. The extended optical piston was designed to be able to observe 57.3% of the combustion chamber area. The extended optical piston was equipped with transparent quartz, and the combustion images were reflected through a 45° angle and

acquired through a high-speed Phantom camera and 105 mm lens. As shown in Fig. 2 (b), the bottom view image could help clarify the development process of the flame surfaces during the MPDF combustion process. Despite these advantages, the optical engine could not be used under a high engine operating load due to inadequate safety. Therefore, optical engine experiments were conducted under only low engine operation load conditions. Skip firing was implemented to avoid damaging the quartz owing to continuous combustion. The MP injection was blocked during the skip firing period, thereby avoiding continuous combustion. After three cycles of continuous combustion, combustion was skipped for nine cycles, and the combustion images were obtained in the last cycle of continuous combustion. Combustion images were captured at 5,400 frame/s, corresponding to one frame per crank angle (CA). Combustion images for 20 cycles per experiment were acquired to decrease the experimental variations. The combustion image acquisition conditions are listed in Table 2.

2.2. Experimental conditions

Table 3 summarizes the reference conditions for the engine experiments. The reference conditions were maintained during the engine experiments. Since marine engines are operated at a lower speed than onshore engines, the engine speed was lowered as much as possible to simulate the speed of marine engines in this study [28]. However, resonance occurred at the engine speeds of 600 RPM to 800 RPM, and severe engine vibration was observed. Therefore, the engine speed of 900 RPM, which is relatively high in the context of marine engines, was determined as the reference condition for engine experiments. According to Azimov et al. [18,29], an extremely small amount of diesel fuel was injected during MPDF combustion. With reference to existing previous research, a preliminary experiment was conducted, and the optimal MP injection quantity was derived. Detailed preliminary experimental results are presented in Appendix A. The lower heating value (LHV) of the MP injection was selected to be 45.8 J/cycle. The intake flow rate of CH₄ gas, which was the main source of energy in this study, was determined considering the intake air flow rate and equivalence ratio.

The experiments in this study could be divided into two parts. First, the intake air flow rate was changed from 500 L/min to 800 L/min in steps of 50 L/min. The corresponding experimental conditions were as listed in Table 4. Because the lambda was set as 2.0, the CH₄ gas flow rate was determined by the intake air flow rate. Moreover, the MP injection timing was varied depending on the intake air flow rate to maintain the same combustion chamber condition at the MP injection timing. As the intake air flow rate increased, the MP injection timing was advanced. The other parameters were maintained constant. Through this experiment, the combustion characteristics were analyzed while the regular premixed combustion changed to PREMIER combustion.

Second, the MP injection timing was varied under two intake air temperatures. Table 5 lists the corresponding engine experimental conditions. In the experiments for the metal engine, the intake air and CH₄ gas flow rates were set as 800 L/min and 42.0 L/min, respectively. At an intake air temperature of 35 °C, the effects on MP injection timing on the misfiring were analyzed. Moreover, the MP injection timing was swept from bTDC 36° to 18° with an interval of CA 3°. In addition, optical engine experiments were performed to analyze the effects of MP injection timing on the misfiring. As mentioned, the optical engine devices could only operate under a low engine operating load. Therefore, the intake air and CH₄ gas flow rates were decreased to 500 L/min and 26.3 L/min, respectively. The intake air temperature was set as 35 °C, and the MP injection timing was swept from bTDC 11° to bTDC 17° and 5° in intervals of CA 3°. Finally, the intake air temperature was increased from 35 °C to 55 °C, and the relationship between the MP injection timing and knocking combustion was investigated. In this condition, the MP injection timing was varied from bTDC 27° to 30° and 24°.

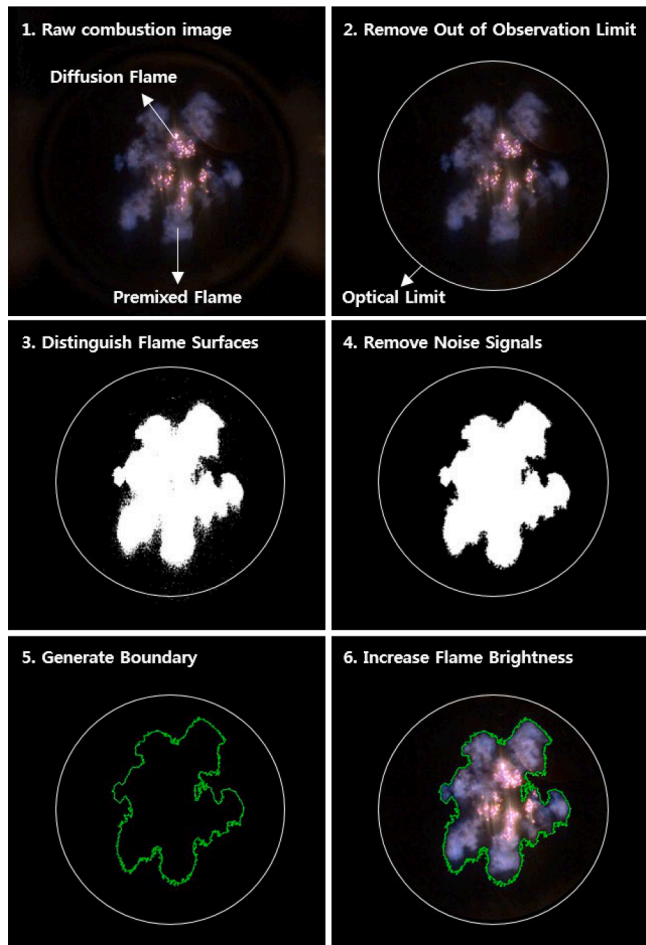


Fig. 3. Postprocessing of combustion images.

2.3. Analysis of the experimental results

In this study, misfiring was defined as the phenomenon in which the cylinder pressure decreased due to a low ignition intensity or disturbance of flame propagation. Conversely, knocking combustion was defined as the phenomenon in which the cylinder pressure increased due to unpredictable autoignition. Misfiring and knocking combustion occurred irregularly, resulting in a high cycle-to-cycle variation. Therefore, the standard deviation of the peak cylinder pressure was calculated to distinguish misfiring and knocking combustion.

In addition, the distributions of the peak cylinder pressure for 100 cycles were compared, and the MPDF combustion forms were quantitatively examined. Under an intake air flow rate of 800 L/min and a CH₄ gas flow rate of 42.0 L/min, the peak cylinder pressure of PREMIER combustion ranged from 170 bar to 220 bar depending on the intake air temperature and MP injection timing. Based on the experimental results, boundaries of misfiring and knocking combustion were defined in terms of the peak cylinder pressures as 160 bar and 230 bar, respectively.

Several researchers have attempted to quantify knocking combustion [30,31]. Among the various knocking combustion indices, the ringing intensity, which indicates the acoustic energy of the resonating pressure wave that creates the sharp sound commonly known as knocking combustion in engines [31–33], was considered in this study. The ringing intensity can be calculated using Eq. (1).

$$\text{Ringing Intensity (MW/m}^2\text{)} = \frac{\sqrt{\gamma RT_{\max}}}{2\gamma P_{\max}} \left[\beta \left(\frac{dP}{dt} \right)_{\max} \right]^2 \quad (1)$$

$\sqrt{\gamma RT_{\max}}$ indicates the speed of sound, and dP/dt represents the

pressure gradient during the combustion period. The coefficient β is the ratio of the pressure pulsation amplitude to the maximum pressure gradient, which is affected by the experiment conditions. In this study, β was varied from 4.0% to 6.0% depending on the experimental conditions. However, because β is a constant value, the average value (0.05) was selected as a representative constant value. γ represents the specific heat ratio. In the engine experiments, the NI-LabVIEW program calculated the ringing intensity by postprocessing the data of the cylinder pressure and intake air temperature. By calculating the ringing intensity values, the MPDF combustion forms could be quantitatively distinguished as each MPDF combustion form exhibited different ringing intensity values.

2.4. Combustion image postprocessing

The combustion images obtained by the optical engine experiment enabled visualization for clarifying the ignition source function and development of flame propagation. In MPDF combustion, both the diffusion flame and premixed flame were simultaneously observed, with each flame exhibiting a different color. To observe the diffusion flame and premixed flame, the natural luminosity was considered instead of detection of OH chemiluminescence through an ultraviolet lens. However, a simple comparison of combustion images under different experimental conditions leads to a limited analysis. To overcome the limitations, this study detected the flame surface boundary and evaluated the flame propagation. A MATLAB program was used to postprocess the raw combustion images, with the steps shown in Fig. 3. First, the outside image of the optical limit was removed. The area of diffusion flame was smaller than that of premixed flame, and most of the premixed flame was dominantly observed during the MPDF combustion period. Therefore, the boundary of flame surfaces was distinguished based on the blue pixel intensity. As the boundary value decreased below a certain value, the noise signal of the flame surfaces dramatically intensified. A blue pixel intensity higher than this value was selected as the boundary value of the flame surfaces. Because the flame brightness varied with the experimental conditions and CA, the boundary values of the flame surfaces were manually determined for all cases. Subsequently, the background noise outside the flame surfaces was removed, and the boundary lines of the flame surfaces were generated. Finally, the brightness of the flame surfaces was increased. Based on the post-processed combustion images, quantitative analyses were performed. The central coordinates of the flame surfaces were derived. In addition, the average flame radius and standard deviation of the flame radius were calculated. The average flame radius was determined using Eq. (2).

$$\text{Averageflameradius(mm)} = \frac{1}{\text{Numberofimagespercycle}} \sum \sqrt{\frac{\text{Flamesurfacearea}}{\pi}} \quad (2)$$

Although combustion images can effectively help analyze experimental results, several factors may lead to experimental errors. In particular, in this study, the boundary of the flame surfaces was manually determined. This method is time-intensive as a large number of combustion images must be processed, and experimental results may vary depending on the boundary value. In addition, the three-dimensional flame surfaces were projected in two dimensions. If the flame surfaces propagate rapidly in the direction normal to the piston, the surfaces may appear distorted at a low flame propagation speed. The experimental error was attempted to be minimized by obtaining combustion images for 20 cycles per experiment.

3. Results and discussion

3.1. Effects of intake air flow rate on MPDF combustion

Effects of intake air flow rate on the MPDF combustion

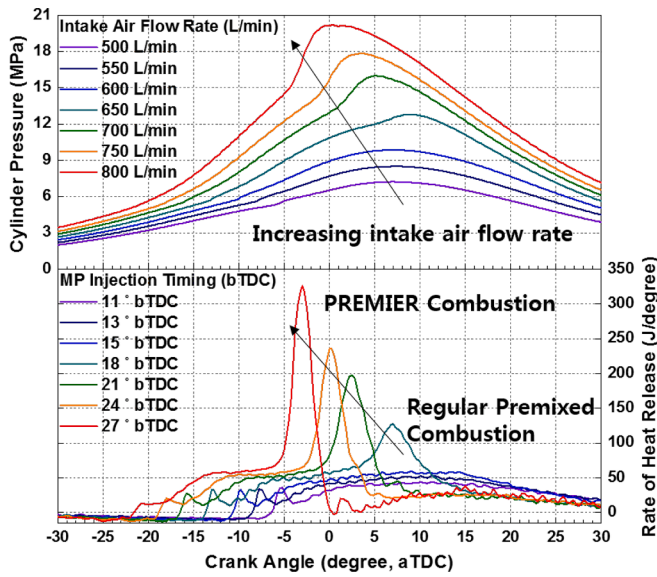


Fig. 4. Effects of intake air flow rate on the cylinder pressure and rate of heat release.

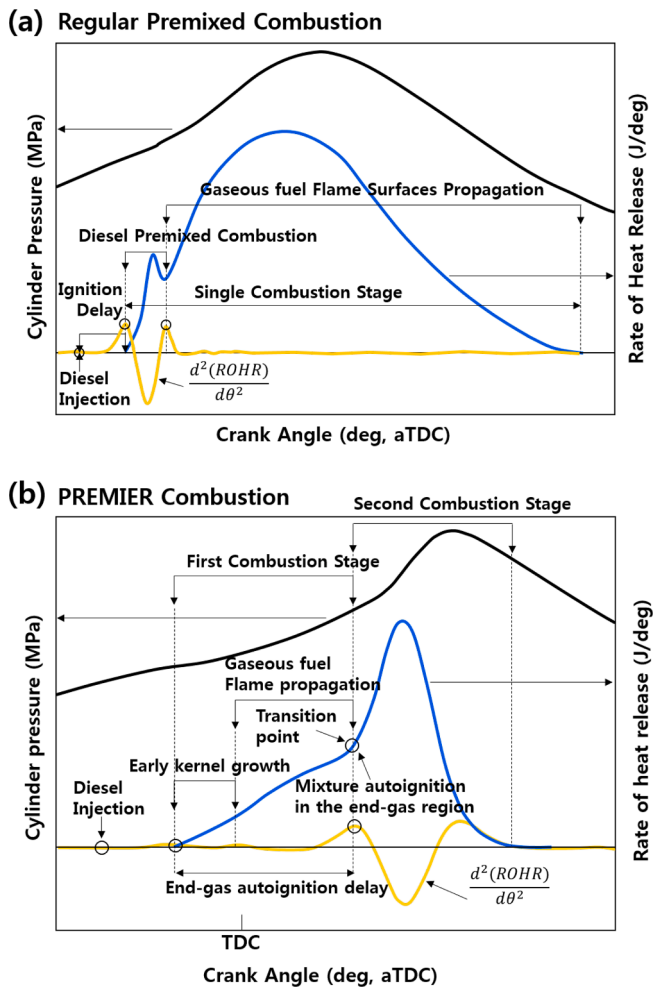


Fig. 5. Schematic of (a) regular premixed combustion and (b) PREMIER combustion [29].

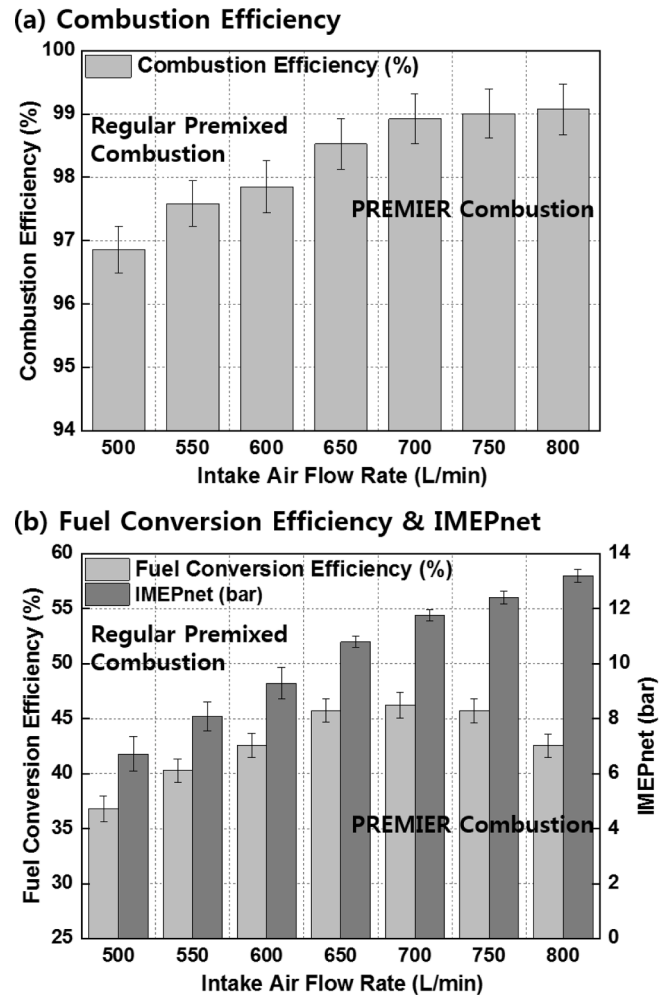


Fig. 6. Effects of intake air flow rate on the (a) combustion efficiency, (b) fuel conversion efficiency and IMEPnet.

characteristics were investigated. The intake air and CH₄ gas flow rates were varied under the same equivalence ratio. As the intake air flow rate increased, the MP injection timing was advanced. Fig. 4 shows the cylinder pressure and rate of heat release for various intake air flow rates and MP injection timing values. Because the lambda was set as 2.0, increasing the intake air flow rate led to a higher cylinder pressure and rate of heat release. Therefore, the MPDF combustion form changed with increasing intake air flow rate. Under a low intake air flow rate, regular premixed combustion corresponded to a relatively low rate of heat release during the combustion period. The cylinder temperature increased in proportion to the intake air flow rate, and a high cylinder temperature affected the reactivity of the end gas. Consequently, autoignition occurred in the end-gas region under a high intake air flow rate, thereby increasing the gradient of the cylinder pressure and rate of heat release. Fig. 5 (a) and (b) indicate regular premixed combustion and PREMIER combustion, respectively [29]. Different combustion forms were observed depending on the occurrence of autoignition. During regular premixed combustion, the diesel fuel was ignited, and the flame surfaces were generated by a mixture of air-gaseous fuel around the ignition point, which propagated to the surrounding region. The flame propagation occupied most of the combustion duration. Unlike regular premixed combustion, which involved a single combustion stage, PREMIER combustion period could be divided into two combustion stages. A moderate combustion intensity was observed in the first combustion stage, i.e., gaseous fuel flame propagation. The first combustion stage switched to the second combustion stage as autoignition occurred in the

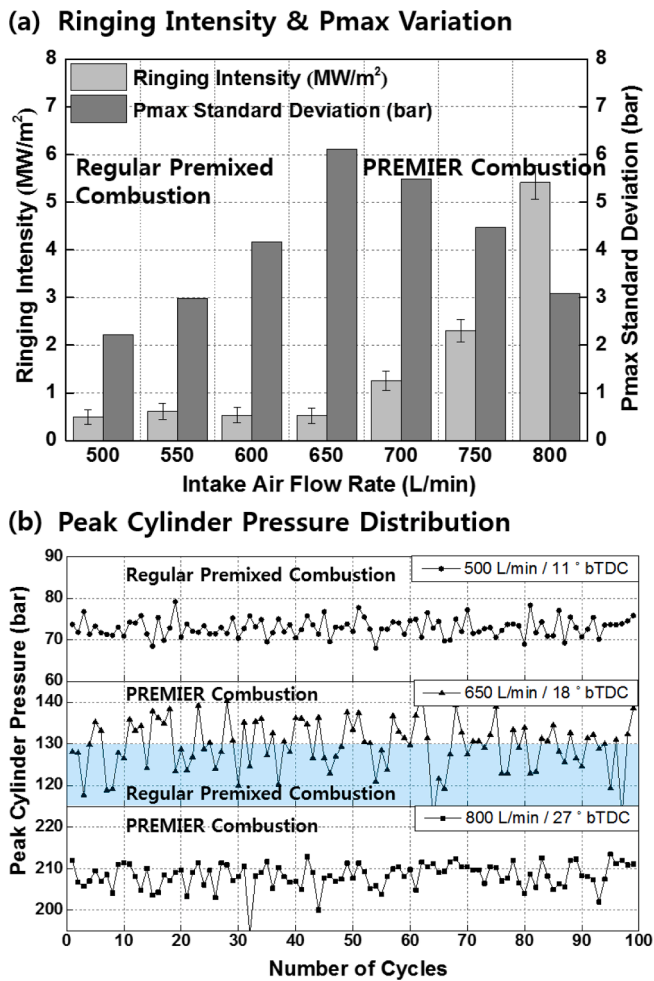


Fig. 7. Effects of intake air flow rate on the (a) ringing intensity, combustion variation, and (b) distributions of peak cylinder pressure.

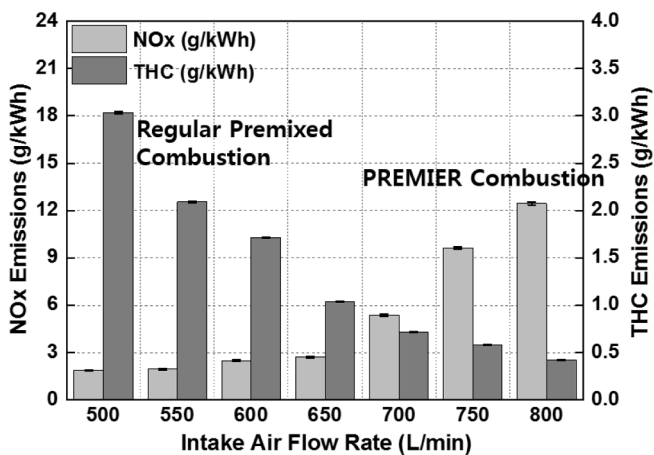


Fig. 8. Effects of intake air flow rate on NOx and THC emissions.

end-gas region. In the second combustion stage, the flame surfaces developed in the ignition spot and collided in the end-gas region, producing a high combustion intensity. Moreover, the change in the MPDF combustion form due to the intake air flow rate considerably influenced the various efficiencies. Fig. 6 (a) and (b) illustrate the effects of the intake air flow rate on various efficiencies and net value of the indicated mean effective pressure (IMEP). Under an intake air flow rate of 500 L/

min, the efficiency values were minimized due to the low combustion temperature of regular premixed combustion. Moreover, because the minimum amount of CH₄ gas was supplied to the combustion chamber, the lowest IMEPnet was observed. As the intake air and CH₄ gas flow rate increased, the IMEPnet steadily increased. In addition, increasing the combustion temperature and decreasing the pumping loss helped increase the combustion efficiency and fuel conversion efficiency until the intake air flow rate of 650 L/min. As the intake air flow rate increased to 700 L/min and more, both efficiencies displayed the opposite trend. In general, the combustion efficiency is related to the formation of incomplete combustion products inside the combustion chamber and proportional to the combustion temperature. As the CH₄ gas flow rate was increased due to the high intake air flow rate under the same equivalence ratio condition, the combustion efficiency appeared to be proportional to the intake air flow rate. In addition, as the combustion temperature increased, the heat loss from the combustion chamber to the piston and combustion chamber wall increased. The advanced MP injection timing advanced the combustion phase. Consequently, most of the combustion occurred before the TDC, producing a large amount of negative work that decreased the engine power. The fuel conversion efficiency was maximized at an intake air flow rate 700 of L/min and decreased as the intake air flow rate increased. Therefore, the intake air flow rate of 700 L/min was the most appropriate condition in terms of fuel conversion efficiencies. However, this condition corresponded to a transition region that existed in both the regular premixed combustion and PREMIER combustion and affected the combustion variation. Fig. 7 (a) illustrates the effects of the intake air flow rate on the ringing intensity and standard deviation of peak cylinder pressure. In general, the ringing intensity indicates the engine operating load. The value exponentially increased after the transient region, as shown in Fig. 7 (a). In other words, the ringing intensity in the case of PREMIER combustion was considerably higher than that under regular premixed combustion. The combustion variation was low under regular premixed combustion. As the combustion form changed from regular premixed combustion to PREMIER combustion, the transient region exhibited the highest combustion variation. After the transient region, the combustion variation reduced under the PREMIER combustion. These results highlighted that the combustion variation is low under the experimental conditions in which regular premixed combustion or PREMIER combustion dominantly appeared. The distributions of the peak cylinder pressure for 100 cycles were compared under three intake air flow rate conditions, as shown in Fig. 7 (b). Under intake air flow rates of 500 of L/min and 800 L/min, regular premixed combustion and PREMIER combustion were observed, respectively. Both combustion forms corresponded to a homogeneous data distribution. In contrast, at the intake air flow rate of 650 L/min, the transient region was observed, involving large differences in the peak cylinder pressure depending on whether autoignition occurred cycle to cycle. This cycle-to-cycle variation led to combustion instability, which adversely influences the engine durability. Although the transient region exhibited a high fuel conversion efficiency, it involved a high combustion variation. Therefore, this condition was not an optimal operating condition. Notably, the intake air flow rate affects the emission gaseous materials and engine performance. In MPDF combustion, an extremely small amount of diesel is injected as an ignition source, and homogeneous gaseous fuel is supplied into the combustion chamber. MPDF combustion thus effectively decreases NOx and PM formation compared to that under diffusion combustion employing diesel fuel [13]. However, a low combustion temperature leads to high THC emissions [9]. Fig. 8 shows trends of the NOx and THC emissions. Extremely low PM emissions were detected by the exhaust gas analyzer, and the trends of PM emissions under various parameters could not be analyzed. The NOx and THC emissions exhibited a trade-off relationship, which was closely related to the cylinder temperature. Unlike regular premixed combustion, PREMIER combustion promoted NOx formation. Therefore, the highest NOx emissions were observed under an intake air flow rate of 800 L/min.

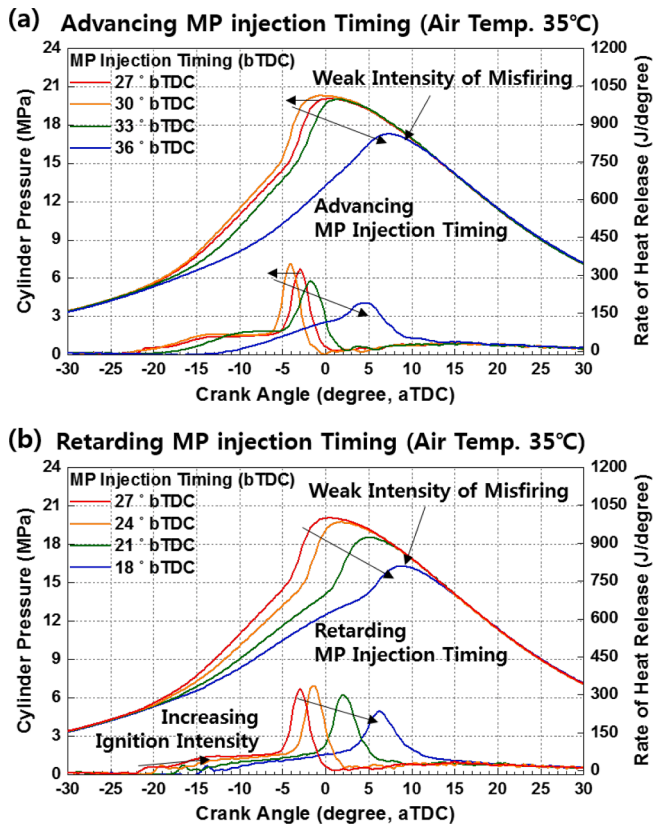


Fig. 9. Effects of (a) advancing and (b) retarding MP injection timing from the reference condition on the cylinder pressure and rate of heat release under an intake air temperature of 35 °C.

3.2. Effects of MP injection timing on MPDF combustion

The MP injection timing is a key parameter influencing the combustion stability. Notably, inappropriate MP injection timing may lead to misfiring and knocking combustion, which can increase the cycle-to-cycle variation. In this study, the intake air and CH₄ gas flow rates were set as 800 L/min and 42.0 L/min, respectively. The MP injection timing was swept under intake air temperatures of 35 °C and 55 °C. These two experimental conditions were selected to compare the effects of MP injection timing on the MPDF combustion characteristics.

3.2.1. Intake air temperature 35 °C

First, the MP injection timing was varied from bTDC 27° to 18° and 36° at intervals of CA 3° under the intake air temperature of 35 °C. Fig. 9 shows the effects of advancing and retarding the MP injection timing on the cylinder pressure and rate of heat release. As shown in Fig. 9 (a), as the MP injection timing advanced from bTDC 27° to 30°, the cylinder pressure increased and the combustion phase was advanced. However, when the MP injection occurred at bTDC 33° and 36°, advancing the MP injection timing led to opposite results since the MP injection timing of bTDC 30° because of misfiring. As shown in Fig. 9 (b), as the MP injection timing was delayed from the reference condition, the cylinder pressure steadily decreased, and misfiring occurred during MP injection at bTDC 18°. These experimental results highlighted that the ratio of misfiring increased by advancing or retarding the MP injection timing from the reference condition under the intake air temperature of 35 °C, but the misfiring caused by advancing and retarding MP injection timing occurred for different reasons. As the MP injection timing advanced, the combustion chamber temperature decreased, thereby increasing the ignition delay. The injected diesel mixed with air and formed a homogeneous mixture, which deteriorated the function of the fuel as the

ignition source. Conversely, retarding the MP injection timing enhanced the ignition intensity due to the high combustion chamber temperature. However, the main combustion occurred during the expansion stroke, which decreased the combustion temperature and led to misfiring. The misfiring in this study corresponded to a low intensity because the cylinder pressure under the misfiring condition was the same as that at the end of the combustion periods. If the MP injection timing was further advanced or retarded from the reference condition, severe misfiring was expected to occur, leading to a decreased cylinder pressure. To validate this analysis for misfiring caused by changing the MP injection timing, combustion images were obtained through the optical engine experiments. To avoid damaging the quartz mounted to acquire the bottom view images, the optical engine was not operated under high engine operating loads. In particular, the engine operating load was decreased by reducing the intake air flow rate to 500 L/min, and the reference MP injection timing condition was delayed to bTDC 11°. Additionally, the MP injection timing was changed from bTDC 11° to bTDC 5° and 17° in intervals of CA 3°. Fig. 10 illustrates the flame propagation process with the MP injection timing. During the ignition delay from aSOE 1° to 5°, the combustion flame was not observed regardless of the MP injection timing. After aSOE 6°, a red diffusion flame, corresponding to diesel fuel, was first observed. Moreover, premixed blue flame surfaces were generated near the ignition point, which propagated to the combustion chamber. The combustion images helped clarify the effects of the MP injection timing on the ignition intensity and flame propagation speed. As the MP injection timing advanced, the size of the ignition flame surfaces decreased. This phenomenon indicated that the ignition intensity decreased under a low cylinder pressure and temperature. Excessively advancing the MP injection timing led to a significant ignition delay, and the injected diesel fuel lost its function as the ignition source. Therefore, misfiring occurred at the timing of ignition. Conversely, an excessively delayed MP injection timing corresponded to a higher ignition intensity and the flame surface development was delayed to after the TDC. The expansion stroke decreased the cylinder pressure and temperature, thereby deteriorating the flame propagation. Therefore, the flame surfaces developed gradually, and misfiring occurred during the late combustion period. To analyze the misfiring phenomena more clearly, the central coordinates of the flame surfaces were calculated from the combustion images. Fig. 11 (a) and (b) illustrate the distributions of the central coordinates flame surfaces for various MP injection timings at aSOE 6° and 22°, respectively. Each data point represents the center coordinate of one cycle, and 20 points are presented for each MP injection timing. In the figure, more widely distributed points correspond to a higher cycle-to-cycle variation.

Fig. 11 (a) shows that advancing the MP injection led to a high cycle-to-cycle variation during ignition owing to low ignition intensity. In contrast, retarding the MP injection increased the cycle-to-cycle variation during the expansion stroke, as shown in Fig. 11 (b). Fig. 12 (a) and (b) shows the quantitative results obtained from combustion images, in terms of the average flame radius and cycle-to-cycle variation with the MP injection timing, respectively. As shown in Fig. 12 (a), advancing the MP injection timing decreased the ignition intensity at the beginning of combustion, and the flame surfaces developed gradually. In contrast, retarding the MP injection suppressed the flame surface development during the late combustion period. Therefore, as shown in Fig. 12 (b), the standard deviation of the flame radius was higher for MP injection timing of bTDC 5°, 8° and 17° than that in the other conditions. The optical engine experiments demonstrated that both advancing and retarding MP injection led to misfiring owing to decrease in the cylinder pressure and temperature during ignition or in the late combustion period, resulting in high cycle-to-cycle variation. Fig. 13 (a) and (b) show that the MP injection timing considerably influenced the various efficiencies and IMEPnet under an intake air temperature of 35 °C. Although the IMEPnet and fuel conversion efficiency exhibit the same trends, the combustion efficiency and fuel conversion efficiency exhibited opposite trends with the MP injection timing. In the reference

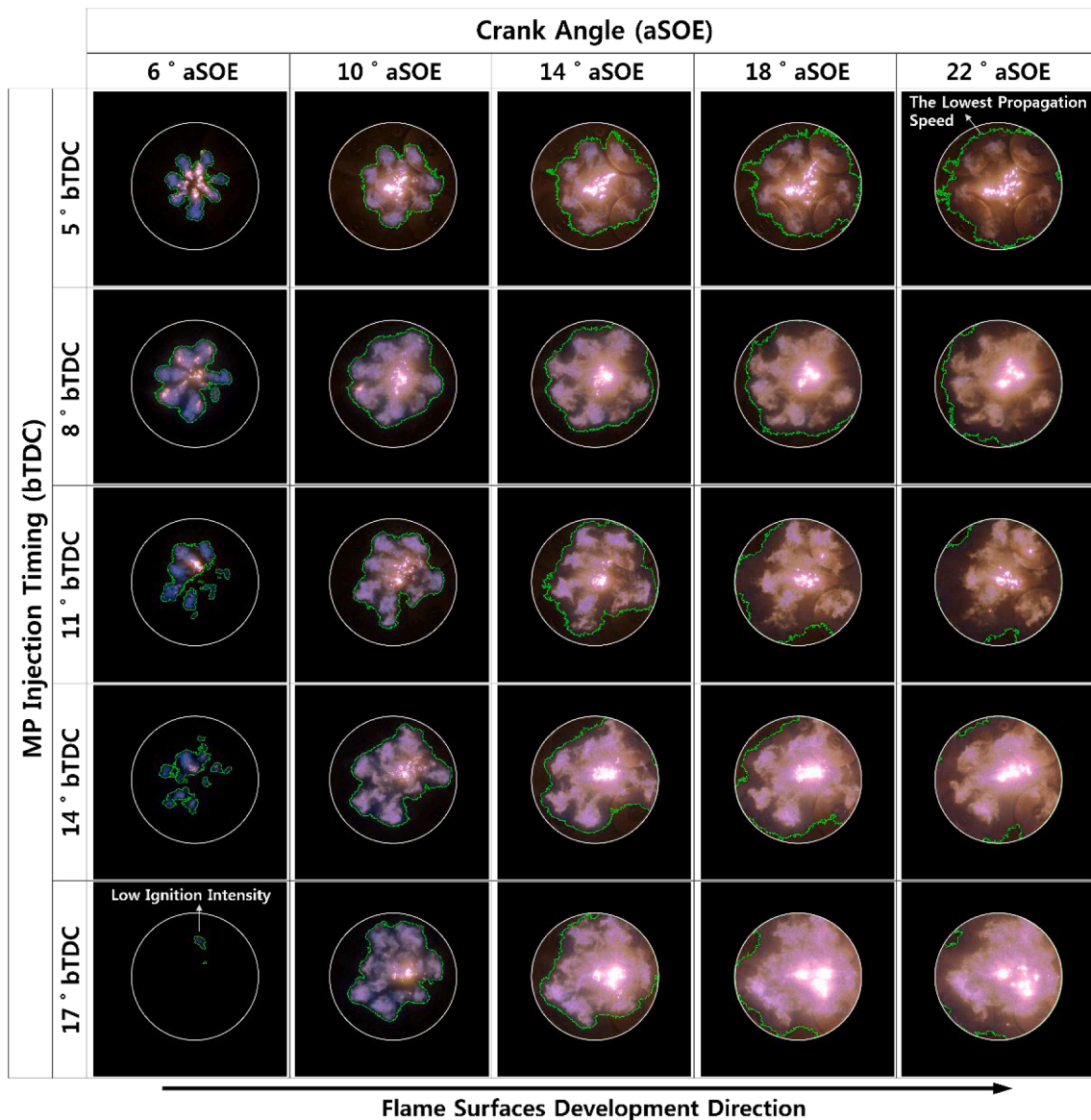


Fig. 10. Effects of MP injection timing on the flame propagation process.

condition involving PREMIER combustion, the highest combustion efficiency could be attributed to the high combustion intensity. This phenomenon also led to advanced combustion, which produced negative work and increased heat loss, resulting in the lowest IMEPnet and fuel conversion efficiency. As the MP injection timing deviated from the reference condition, a lower combustion efficiency was observed. Advancing and retarding the MP injection from the reference condition increased the IMEPnet and fuel conversion efficiency by decreasing the heat loss and negative work despite the low combustion efficiency. As mentioned, because a low level of misfiring occurred under the MP injection timing of bTDC 36° and 18°, the IMEPnet and fuel conversion efficiency increased. If the MP injection timing was further advanced or retarded from the reference condition, severe misfiring was expected to occur, which could significantly deteriorate the engine performances. In addition to the engine performances, the combustion variation varied with the MP injection timing. Fig. 14 (a) shows the effects of the MP injection timing on the ringing intensity and standard deviation of the peak cylinder pressure. The two values exhibited a trade-off relationship. As the MP injection timing deviated from the reference condition, misfiring occurred, which simultaneously decreased the ringing intensity and increased the combustion variation. To analyze the

PREMIER combustion and misfiring, distributions of the peak cylinder pressure under the MP injection timing of bTDC 36°, 27° and 18° were compared, as shown in Fig. 14 (b). In the reference condition, corresponding to PREMIER combustion, the highest peak cylinder pressure was observed, along with the minimum cycle-to-cycle variation. In the other conditions shows, the peak cylinder pressure decreased irregularly owing to misfiring, and thus, the cycle-to-cycle combustion variation increased, leading to combustion instability. The NO_x and THC emission levels shown in Fig. 15 support these experimental results. The NO_x and THC emissions exhibited a trade-off relationship. A more advanced combustion phase corresponded to a higher amount of NO_x emissions. Moreover, the THC emissions mainly increased under the misfiring conditions.

3.2.2. Intake air temperature of 55 °C

The intake air temperature was increased to 55 °C, and the MP injection timing was varied from bTDC 27° to 30° and 24°. Fig. 16 (a) and (b) show the effects of MP injection timing on the cylinder pressure and rate of heat release under intake air temperatures of 35 °C and 55 °C, respectively. As the MP injection timing was retarded from bTDC 30° to 24°, the cylinder pressure decreased and the rate of heat release was

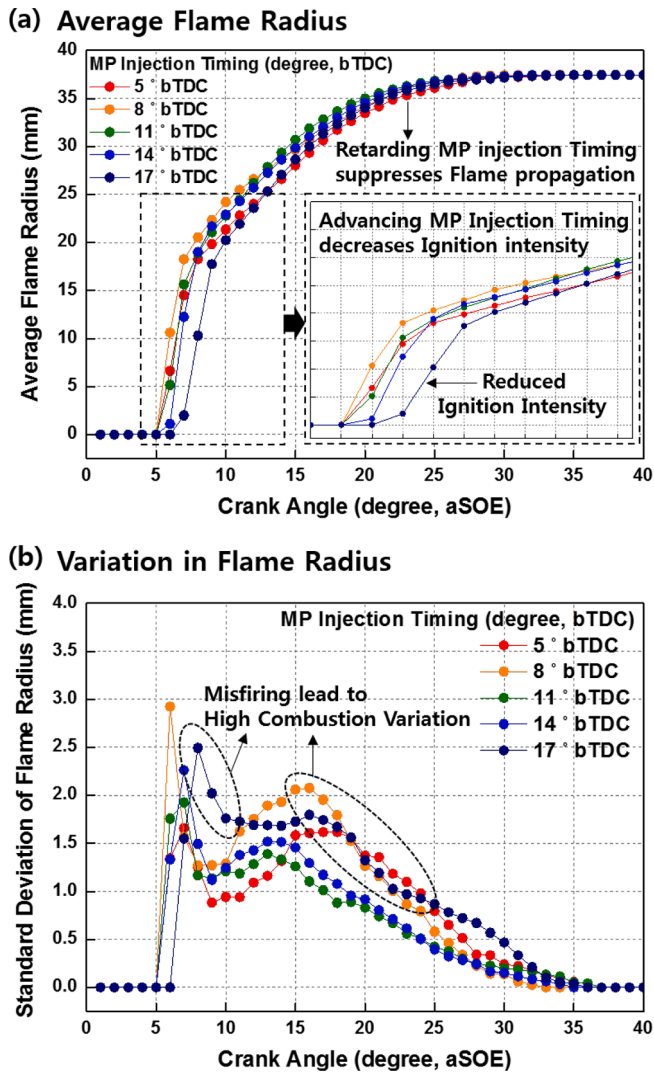


Fig. 11. Distributions of central coordinates of flame surfaces under misfiring caused by (a) advancing and (b) retarding MP timing.

maintained when the intake air temperature was 35 °C. In contrast, when the MP injection was retarded at an intake air temperature at 55 °C, the cylinder pressure and rate of heat release increased, and knocking combustion occurred under the MP injection timing of bTDC 24°. The results demonstrated that retarding the MP injection timing led to knocking combustion under a high intake air temperature. Notably, as the MP injection was delayed, increasing the combustion chamber temperature led to unpredictable autoignition, and the flame surfaces originating from the autoignition point and ignition source collided. The shockwave generated in this process led to a significant amount of engine noise and vibration, corresponding to knocking combustion. To further analyze the knocking combustion characteristics, the effects of MP injection timing on the mass fraction burned (MFB) for an intake air temperature of 55 °C were examined, as shown in Fig. 17. According to this figure, MPDF combustion could be divided into several groups depending on the MFB. First, the ignition delay was defined as CA00-10, corresponding to CA from aSOE to 10.0 % of MFB. The durations of main combustion and residual gas combustion were defined as CA10-70 and CA 70-90, respectively. Because the residual gas combustion periods were similar at all experimental conditions, only the ignition delay and main combustion period were considered. First, CH₄ gas absorbed the heat energy in the combustion chamber until the start of flame propagation. A more retarded MP injection timing corresponded to a higher heat energy absorbed by CH₄ gas. This phase corresponded to the

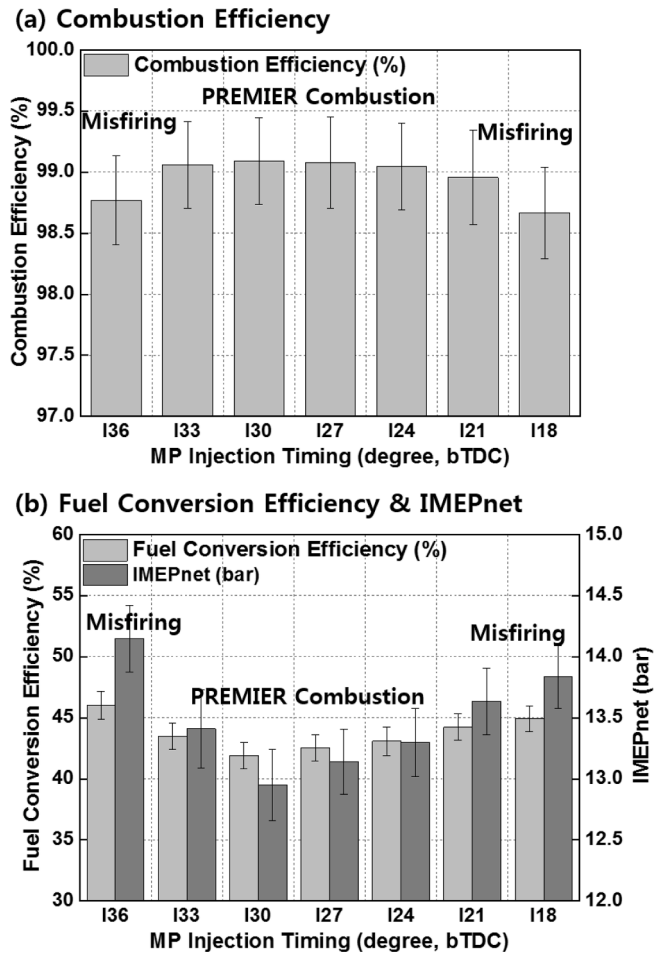


Fig. 12. Effects of MP injection timing on the (a) flame radius and (b) variation in combustion images.

maximum time to reach MFB 10.0 % when the MP injection timing was bTDC 24°. Knocking combustion occurred in this condition, and the main combustion period was significantly reduced. Consequently, the main combustion duration exhibited a trend opposite to that of the ignition delay. Fig. 18 (a), (b) and (c) compare the effects of MP injection timing on the various efficiencies and IMEPnet under intake air temperatures of 35 °C and 55 °C. Because misfiring did not occur in the MP injection timing of bTDC 30° to 24°, the combustion efficiency did not differ with the MP injection timing, and the combustion efficiency was proportional only to the intake air temperature. Although the fuel conversion efficiency could be enhanced by retarding the MP injection timing when the intake air temperature was 35 °C, increasing the intake air temperature led to knocking combustion when MP injection timing was retarded, and the negative work and heat loss increased. Therefore, the difference in the fuel conversion efficiency with the intake air temperature increased as the MP injection timing was delayed. As shown in Fig. 18 (b) and (c), the trend of the IMEPnet with the MP injection timing at intake air temperatures of 35 °C and 55 °C was the same as that of the fuel conversion efficiency. Knocking combustion occurred randomly, and the cylinder pressure was considerably increased owing to the knocking combustion, thereby deteriorating the combustion stability. Fig. 19 (a) shows the ringing intensity and standard deviation of the peak cylinder pressure with the MP injection timing for the intake air temperature of 55 °C. As the MP injection timing was delayed, the ringing intensity and combustion variation increased; this trend was closely related to the occurrence of knocking combustion. Fig. 19 (b) shows the distributions of peak cylinder pressure for various MP injection timings under the intake air temperature of 55 °C. Most of the peak

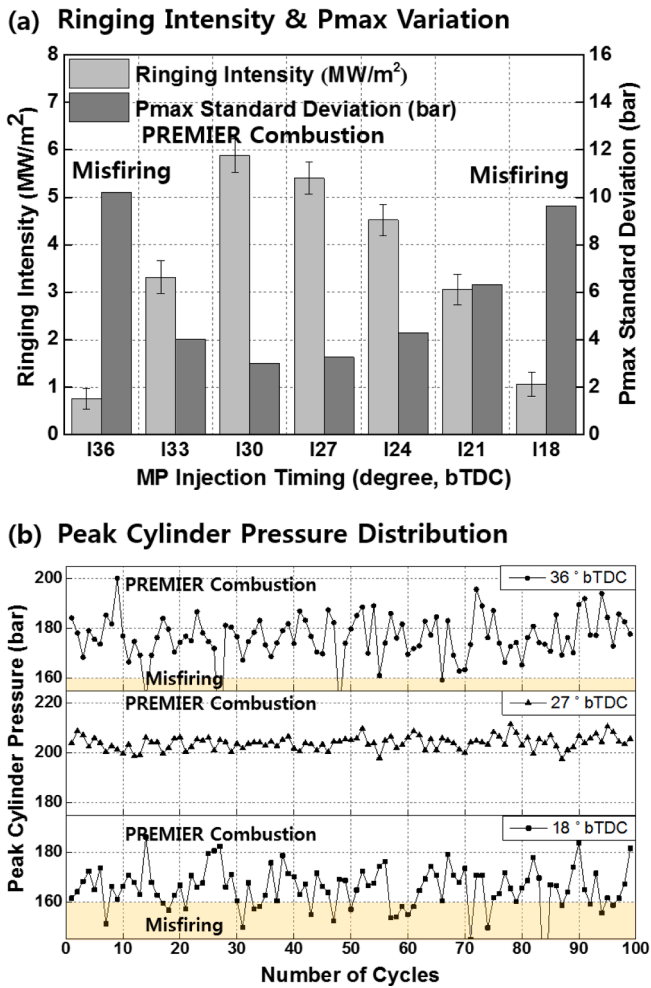


Fig. 13. Effects of MP injection timing on the (a) combustion efficiency, (b) IMEPnet and fuel conversion efficiency under intake air temperature 35 °C.

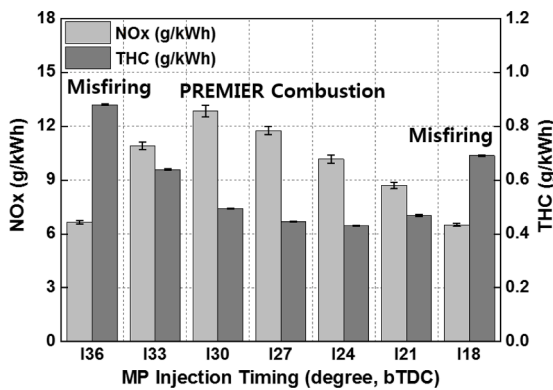


Fig. 14. Effects of MP injection timing on the (a) ringing intensity, combustion variation and (b) distributions of peak cylinder pressure under an intake air temperature of 35 °C.

cylinder pressure data were located in the PREMIER combustion region under the MP injection timing of bTDC 30°. A more retarded MP injection timing corresponded a higher shift in the peak cylinder pressure toward the knocking combustion region. The occurrence of knocking combustion with the MP injection timing also influenced the NOx and THC emissions. Fig. 20 shows the experimental results for the MP injection timing of bTDC 30° and 27°. Retarding the MP injection timing simultaneously decreased the NOx emissions and increased the THC emissions. Knocking combustion occurred under the MP injection timing

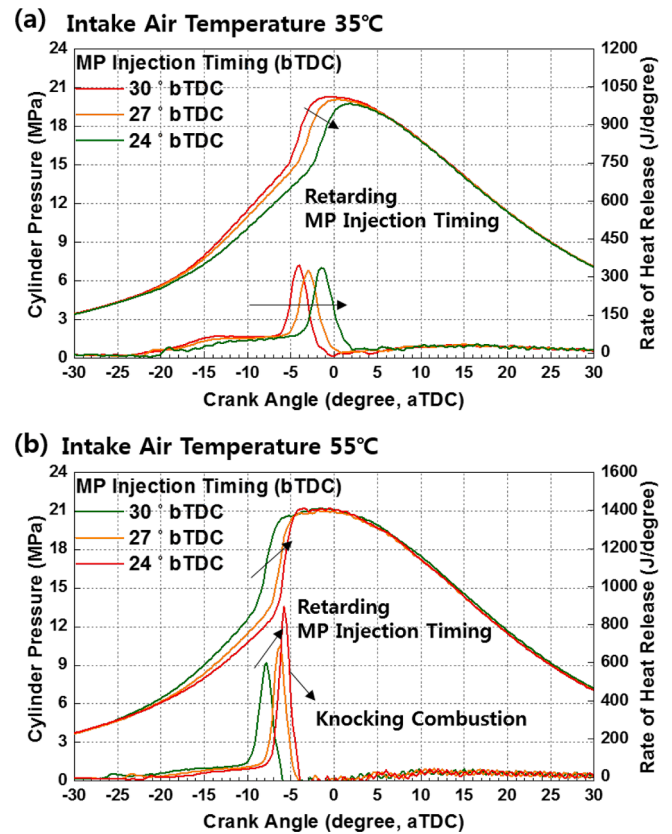


Fig. 15. Effects of MP injection timing on the NOx and THC emissions under an intake air temperature of 35 °C.

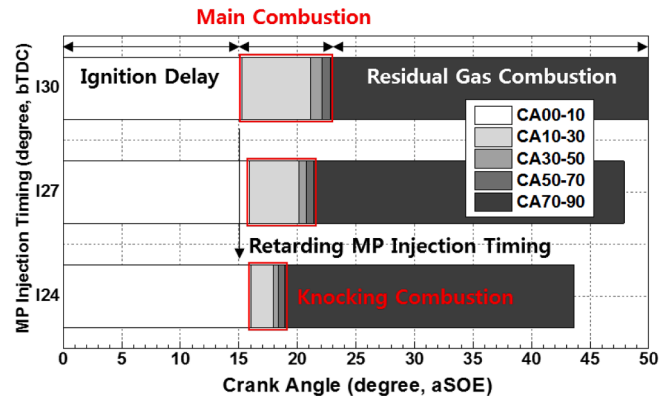


Fig. 16. Comparison of effects of retarding MP injection timing on the cylinder pressure and rate of heat release under an intake air temperature of (a) 35 °C and (a) 55 °C.

of bTDC 24°, which promoted NOx formation and oxidation of incomplete combustion materials. Through the engine experiments, it was confirmed that retarding the MP injection timing led to knocking combustion under a high intake air temperature.

3.3. Summarization of MPDF combustion form and characteristics

Notably, the experimental results demonstrated that the MPDF combustion forms changed depending on the engine operating conditions. Fig. 21 shows the distributions of the experimental results with respect to the ringing intensity and combustion variation. The blue marked points indicate the trends of the intake air flow rate experiment. Regular premixed combustion, which corresponded to the lowest ringing intensity and combustion variation, occurred at the intake air flow

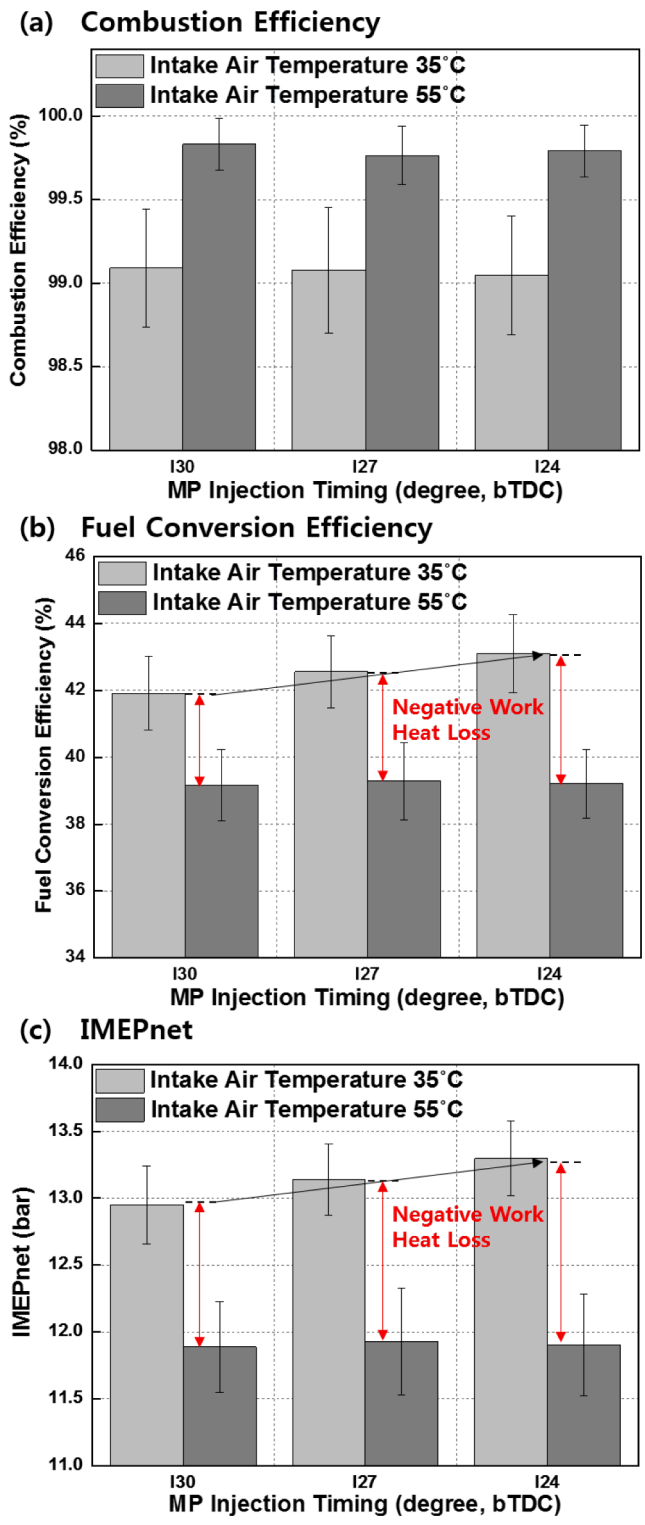


Fig. 17. Effects of MP injection timing on the MFB under the intake air temperature 55 °C.

rate of 500 L/min. As the intake air flow rate increased, the regular premixed combustion transformed to the PREMIER combustion through the transient region. Since both combustion forms coexisted, the combustion variation increased sharply in the transient region. After the transient region, the regular premixed combustion changed completely to the PREMIER combustion, and the combustion variation steadily reduced. The black marked points indicate the experimental results for various intake air temperatures and MP injection timing values for an

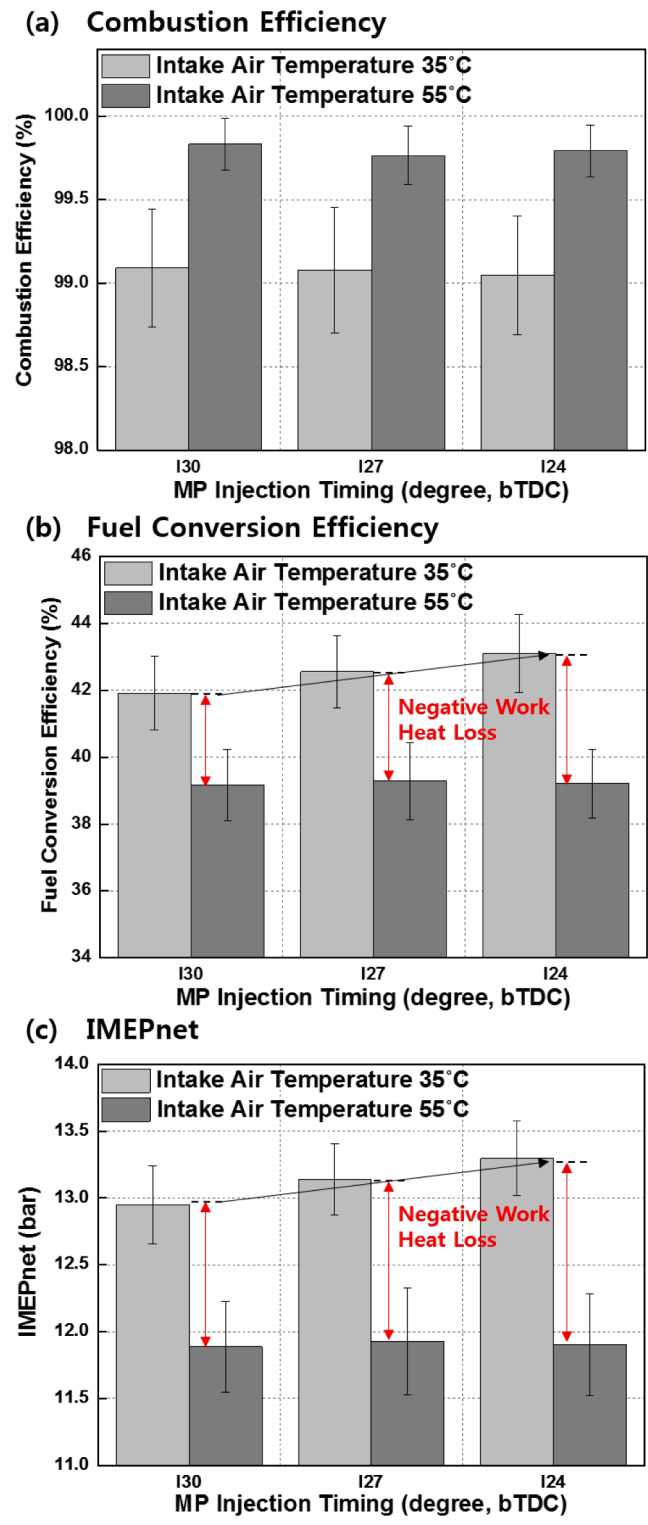


Fig. 18. Effects of MP injection timing on the (a) combustion efficiency, (b) fuel conversion efficiency and (c) IMEPnet under intake air temperatures of 35 °C and 55 °C.

intake air flow rate of 800 L/min. The experimental results could be divided into three regimes in accordance with the ringing intensity, and various MPDF combustion forms were observed in each regime. The reference condition located in the middle regime corresponded to the lowest combustion variation due to the PREMIER combustion. However, change the engine operating parameters led to misfiring or knocking combustion, and the experimental results shifted to other regimes. In

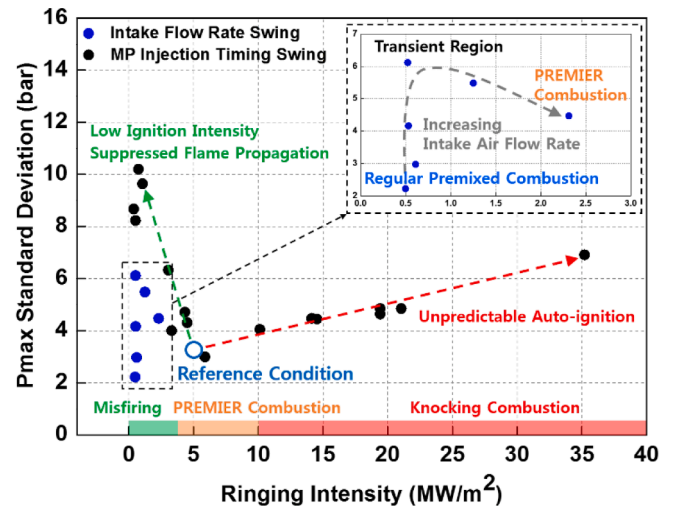
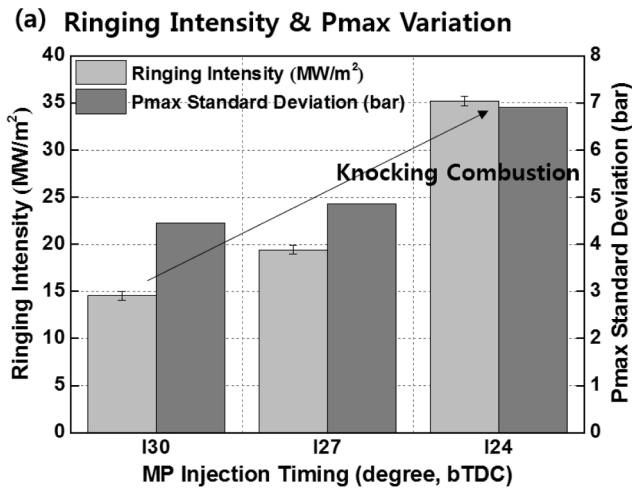


Fig. 21. Distributions of experimental results in terms of the ringing intensity and combustion variation.

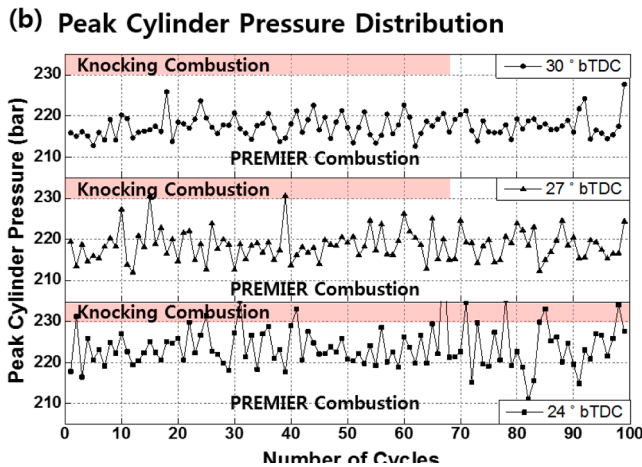


Fig. 19. Effects of MP injection timing on (a) ringing intensity, combustion variation and (b) distributions of peak cylinder pressure under intake air temperature 55 °C.

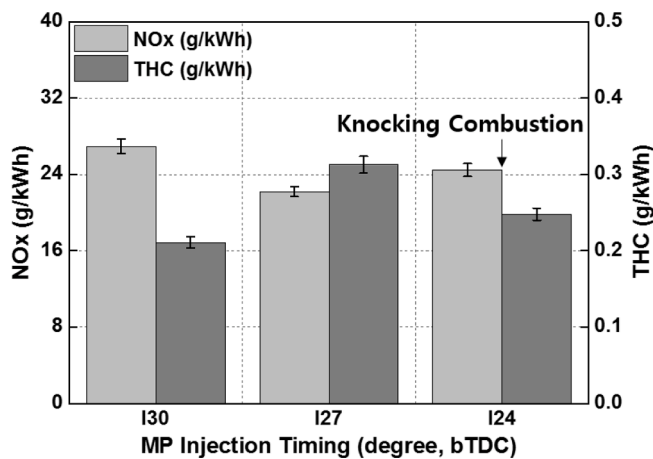


Fig. 20. Effects of MP injection timing on the NOx and THC emissions under an intake air temperature of 55 °C.

particular, misfiring mainly occurred under a low ignition intensity and suppressed flame propagation, corresponding to a low ringing intensity and high combustion variation. Unpredictable autoignition contributed to knocking combustion and increased the combustion variation and ringing intensity. Among the various MPDF combustion forms, regular premixed combustion and PREMIER combustion corresponded to the lowest combustion variation. In particular, in PREMIER combustion, the

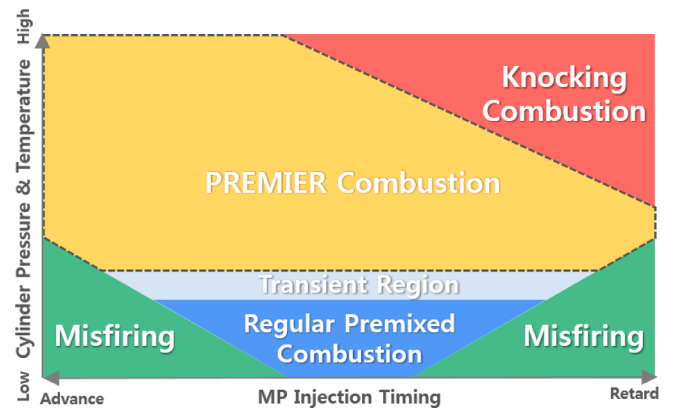


Fig. 22. Regions of various MPDF combustion forms with respect to MP injection timing and cylinder pressure and temperature.

low combustion variation was observed even under high cylinder pressures of approximately 170 bar to 220 bar. Therefore, the PREMIER combustion corresponded to the optimal engine operating conditions for marine engines. Moreover, it was deemed necessary to appropriately modify the MP injection timing in accordance with the cylinder conditions to maintain the PREMIER combustion. The effects of MP injection timing, cylinder pressure and temperature on the MPDF combustion forms are shown in Fig. 22. The findings can be used to derive strategies for avoiding misfiring and knocking combustion. As well as the parameters that focused on this study, the region of the PREMIER combustion could be expanded by modifying other parameters such as MP injection pressure, quantity and composition of gaseous fuel. High MP injection pressure, quantity and adding the hydrocarbon gases could effectively prevent misfiring. Conversely, high EGR rate or adding CO₂ gas in the combustion chamber could suppress the knocking combustion by decreasing the combustion temperature.

As mentioned, the PREMIER combustion was identified as the optimal engine operating conditions in terms of engine performances. However, because marine engines must adhere to emissions regulations, the limits of PREMIER combustion in terms of the emissions must be clarified. Among various emissions materials, MPDF combustion rarely leads to the formation of SOx and PM because most of the energy is derived by CH₄ gas. Therefore, PREMIER combustion can easily satisfy the emissions regulations, except for those associated with NOx emissions. Although the NOx emissions in MPDF combustion are less than those under diesel combustion, the generation of NOx, mainly in the high-temperature region in the combustion chamber, is a critical

disadvantage under PREMIER combustion. The strictest emissions regulations (Tier III) that have been in effect since January 1, 2016 limit the NOx emissions depending on engine speed for marine engines with an output of over 130 kW in the ECA [6,7]. According to the emissions regulations, the maximum allowable NOx emission level at engine speed of 900 RPM is 2.31 g/kWh. In this study, only the conditions associated with the intake air flow rates of 500 L/min and 550 L/min satisfy the NOx emissions regulations. In this context, it is necessary install an aftertreatment system such as selective catalyst reduction to reduce the NOx emissions under the PREMIER combustion condition.

4. Conclusions

This study was aimed at analyzing the effects of intake air conditions and MP injection timing on the characteristics of MPDF combustion. The optimal engine operating conditions were derived to reduce the combustion variation. The following conclusions were derived.

1. Increasing the intake air flow rate leads to autoignition in the end-gas region and transforms the regular premixed combustion to the PREMIER combustion. Despite autoignition in the end-gas region, the PREMIER combustion exhibits a low combustion variation. High combustion variation is observed in the transient region in which regular premixed combustion and PREMIER combustion coexist.
2. Under an intake air temperature of 35 °C, advancing and retarding the MP injection lead to misfiring owing to the decreased cylinder pressure and temperature at the time of ignition or in the late combustion period, leading to high combustion variation. As the intake air temperature increases to 55 °C, retarding the MP injection timing leads to knocking combustion. Misfiring and knocking combustion increase the combustion variation, thereby deteriorating the combustion stability.
3. The MPDF combustion forms can be classified in accordance with the ringing intensity. Regular premixed combustion and misfiring occur in the low ringing intensity regime. Although regular premixed combustion corresponds to a low combustion variation, misfiring leads to a high combustion variation. PREMIER combustion, which occurs in the middle ringing intensity regime exhibits a low combustion variation. Knocking combustion occurs in the high ringing intensity regime and leads to a high combustion variation.
4. Because the PREMIER combustion can exhibit a low combustion variation even under a high cylinder pressure, it corresponds to the optimal engine operating condition in terms of the engine performances. However, PREMIER combustion yields a large amount of NOx emissions. Therefore, it is necessary to install an aftertreatment system for satisfying the emissions regulations for marine engines.

CRediT authorship contribution statement

Minho Choi: Experiments, Writing – original draft, Conceptualization, Methodology, Investigation. **Sungwook Park:** Writing – review & editing, Supervision.

Declaration of Competing Interest

The authors declare that they have no known competing financial interests or personal relationships that could have appeared to influence the work reported in this paper.

Acknowledgments

This work was supported by the BK21 FOUR program from the National Research Foundation and Ministry of Education and the Korea Evaluation Institute of Industrial Technology (20015914).

Appendix A

Before performing this study, the optimal MP injection quantity was derived. Table A1 summarizes the experimental conditions to optimize the MP injection quantity. The injector was controlled using a solenoid signal, and the MP injection duration was changed from 0.23 ms to 0.40 ms. Other conditions were maintained. Fig. A.1 shows the cylinder pressure and rate of heat release in accordance with the MP injection durations. As the MP injection duration increased, the ignition delay decreased and the cylinder pressure and rate of heat release increased. However, results for the MP injection durations of 0.30 ms and 0.40 ms indicated that the ignition delay, cylinder pressure and rate of heat release did not change significantly with the MP injection duration. Fig. A.2 shows the effects of MP injection duration on the ringing intensity and combustion variation. It was noted that the MP injection duration was required to be higher than 0.30 ms to maintain stable combustion. Therefore, the MP injection duration of 0.30 ms, corresponding to the LHV of 45.8 J/cycle, was selected as the optimal condition.

Table A1

Experimental conditions for optimizing the MP injection quantity.

Item	Description
Engine Type	Metal Engine
Intake Air Flow Rate (L/min)	800
CH ₄ Gas Flow Rate (L/min)	42.0
Intake Air Temperature (°C)	35
MP Injection Timing (CA, bTDC)	27
MP Injection Duration (ms)	0.23, 0.27, 0.30, 0.40

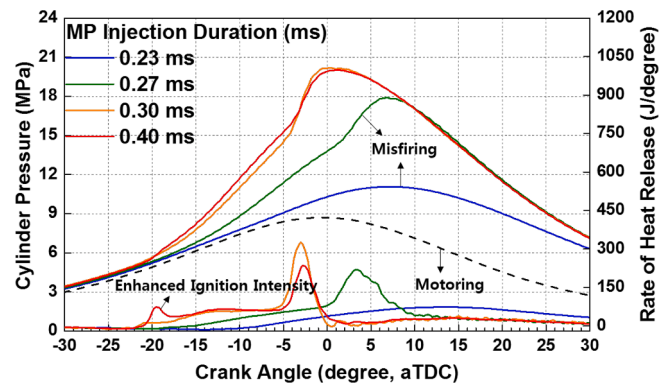


Fig. A1. Effects of MP injection duration on the cylinder pressure and rate of heat release.

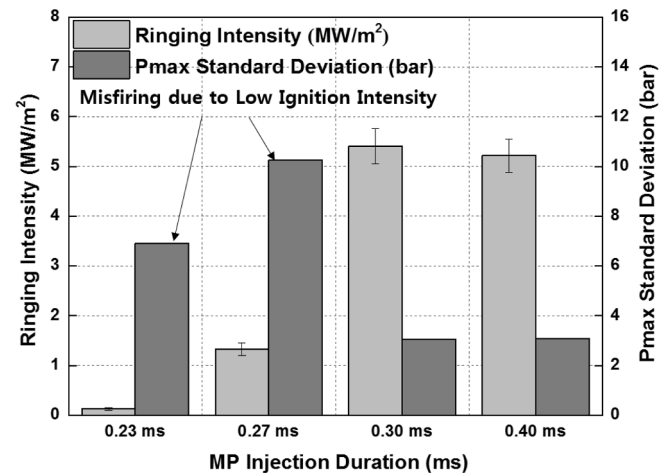


Fig. A2. Effects of MP injection duration on the ringing intensity and combustion variation.

References

- [1] Funayama Y, Nakajima H, Shimokawa K. A study on the effects of a higher compression ratio in the combustion chamber on diesel engine performance. *SAE Int* 2016.
- [2] Heywood JB. *Internal combustion engine fundamentals*. McGraw-Hill Education; 2018.
- [3] Naber JD, Johnson JE. *Internal combustion engine cycles and concepts*. In: Folkson R, editor. *Alternative fuels and advanced vehicle technologies for improved environmental performance*. Woodhead Publishing; 2014. p. 197–224.
- [4] Schnurr REJ, Walker TR. *Marine transportation and energy use. Reference module in earth systems and environmental sciences*; Elsevier. In: *Reference Module in Earth Systems and Environmental Sciences*. Elsevier; 2019. <https://doi.org/10.1016/B978-0-12-409548-9.09270-8>.
- [5] M.A. Ghadikolaei, C.S. Cheung, K.-F. Yung. Study of performance and emissions of marine engines fueled with liquefied natural gas (LNG). *Proceedings of 7th PAAMES and AMEC2016*. 13 (2016) 14.
- [6] Herdzik J. Emissions from marine engines versus IMO certification and requirements of tier 3. *J KONES*. 2011;18:161–7.
- [7] Čampara L, Hasanspahić N, Vujičić S. Overview of MARPOL ANNEX VI regulations for prevention of air pollution from marine diesel engines. *SHS Web Conf*. 2018;58: 01004.
- [8] Zheng J, Wang J, Zhao Z, Wang D, Huang Z. Effect of equivalence ratio on combustion and emissions of a dual-fuel natural gas engine ignited with diesel. *Appl Therm Eng* 2019;146:738–51.
- [9] Imtenan S, Varman M, Masjuki HH, Kalam MA, Sajjad H, Arbab MI, et al. Impact of low temperature combustion attaining strategies on diesel engine emissions for diesel and biodiesels: A review. *Energy Convers Manage* 2014;80:329–56.
- [10] Karim GA. *Dual-fuel diesel engines*. CRC Press; 2015.
- [11] Ahmad Z, Aryal J, Ranta O, Kaario O, Vuorinen V, Larmi M. An optical characterization of dual-fuel combustion in a heavy-duty diesel engine. *SAE International* 2018.
- [12] Aydin K. Effect of engine parameters on cyclic variations in spark ignition engines. In: *6th International Advanced Technologies Symposium (IATS'11)*; 2011. p. 57–63.
- [13] Choi M, Mohiuddin K, Park S. Effects of methane ratio on MPDF (micro-pilot dual-fuel) combustion characteristic in a heavy-duty single cylinder engine. *Sci Rep* 2021;11:9740.
- [14] Duraisamy G, Rangasamy M, Nagarajan G. Effect of EGR and premixed mass percentage on cycle to cycle variation of methanol/diesel dual fuel RCCI Combustion. *SAE Int* 2019.
- [15] Maurya RK, Agarwal AK. Experimental study of combustion and emission characteristics of ethanol fuelled port injected homogeneous charge compression ignition (HCCI) combustion engine. *Appl Energy* 2011;88:1169–80.
- [16] Maurya RK, Agarwal AK. Experimental investigation on the effect of intake air temperature and air–fuel ratio on cycle-to-cycle variations of HCCI combustion and performance parameters. *Appl Energy* 2011;88:1153–63.
- [17] Lee J, Chu S, Kang J, Min K, Jung H, Kim H, et al. Operating strategy for gasoline/diesel dual-fuel premixed compression ignition in a light-duty diesel engine. *Int J Automot Technol* 2017;18:943–50.
- [18] Azimov U, Tomita E, Kawahara N, Harada Y. Premixed mixture ignition in the end-gas region (PREMIER) combustion in a natural gas dual-fuel engine: operating range and exhaust emissions. *Int J Engine Res* 2011;12:484–97.
- [19] Kawahara N, Kim Y, Wadahama H, Tsuboi K, Tomita E. Differences between PREMIER combustion in a natural gas spark-ignition engine and knocking with pressure oscillations. *Proc Combust Inst* 2019;37:4983–91.
- [20] Poonia MP, Ramesh A, Gaur RR. Effect of intake air temperature and pilot fuel quantity on the combustion characteristics of a LPG diesel dual fuel engine. *SAE International* 1998.
- [21] Meng X, Tian H, Zhou Y, Tian J, Long W, Bi M. Comparative study of pilot fuel property and intake air boost on combustion and performance in the CNG dual-fuel engine. *Fuel* 2019;256:116003.
- [22] Tomita E, Harada Y, Kawahara N, Sakane A. Effect of EGR on combustion and exhaust emissions in supercharged dual-fuel natural gas engine ignited with diesel fuel. *SAE International* 2009.
- [23] Aksu C, Kawahara N, Tsuboi K, Nanba S, Tomita E, Kondo M. Effect of hydrogen concentration on engine performance, exhaust emissions and operation range of PREMIER combustion in a dual fuel gas engine using methane-hydrogen mixtures. *SAE Int* 2015.
- [24] Valipour Berenjestanaki A, Kawahara N, Tsuboi K, Tomita E. End-gas autoignition characteristics of PREMIER combustion in a pilot fuel-ignited dual-fuel biogas engine. *Fuel* 2019;254:115634.
- [25] Shim E, Park H, Bae C. Intake air strategy for low HC and CO emissions in dual-fuel (CNG-diesel) premixed charge compression ignition engine. *Appl Energy* 2018; 225:1068–77.
- [26] Mazloomi K, Gomes C. Hydrogen as an energy carrier: Prospects and challenges. *Renew Sustain Energy Rev* 2012;16(5):3024–33.
- [27] Topinka JA, Gerty MD, Heywood JB, Keck JC. Knock Behavior of a Lean-Burn, H₂ and CO enhanced, SI gasoline engine concept. *SAE Int* 2004.
- [28] Li J, Wu B, Mao G. Research on the performance and emission characteristics of the LNG-diesel marine engine. *J Nat Gas Sci Eng* 2015;27:945–54.
- [29] U. Azimov, E. Tomita, N. Kawahara. Combustion and exhaust emission characteristics of diesel micro-pilot ignited dual-fuel engine. *Diesel engine—combustion, emissions and condition monitoring*. (2013) 33–62.
- [30] Lounici MS, Benbellil MA, Loubar K, Niculescu DC, Tazerout M. Knock characterization and development of a new knock indicator for dual-fuel engines. *Energy*. 2017;141:2351–61.
- [31] Eng JA. Characterization of pressure waves in HCCI combustion. *SAE Int* 2002.
- [32] Maurya RK, Saxena MR. Characterization of ringing intensity in a hydrogen-fueled HCCI engine. *Int J Hydrogen Energy* 2018;43:9423–37.
- [33] Sjöberg M, Dec JE. Effects of engine speed, fueling rate, and combustion phasing on the thermal stratification required to limit HCCI knocking intensity. *SAE Int* 2005.